Analysis of maximum arching conditions in active plane-strain trapdoors in sand

Ashraf S Osman[1] and SW Jacobsz[2]

Abstract

The trapdoor problem is a useful model to understand the stress distribution around geo-structures. This paper focuses on evaluating the conditions of maximum arching (minimum loads on trapdoors) developing during the lowering of plane-strain active trapdoors in cohessionless granular materials. A parametric study using finite element analysis has been performed to investigate various factors affecting the maximum arching conditions in active trapdoors, with a particular focus on the effect of soil dilatancy. The paper also presents rigorous upper bound limit analysis solutions. Previously published solutions dealing with soil non-associativity have been discussed and compared with the finite element results. The finite element analysis shows that using a Mohr Column model with the associative flow rule and reduced strength parameters, overestimates the load reduction on trapdoors compared with a non-associative model with full soil strength parameters.

[1] Department of Engineering, Durham University, South Road, Durham DH1 3LE, UK.
Tel: +44 191 3342425 Email: ashraf.osman@durham.ac.uk

[2] Department of Civil Engineering, Faculty of Engineering, Built Environment and Information Technology, University of Pretoria, Hatfield 0028, South Africa.
Tel +27 12 420 3124, Email sw.jacobsz@up.ac.za

1. Introduction

The classical trapdoor problem provides a useful tool to understand the stress redistribution occurring around geotechnical structures such as tunnels, buried pipes, retaining structures, pile-supported embankments and plate anchors. It could also be useful to provide insight into the process of cavity propagation towards the surface resulting in sinkhole formation. The experimental setup usually comprises a horizontal trapdoor below a geomaterial with downward (active) or upward (passive) movement of the trapdoor to model the deflection of support relative to the adjacent soil mass. The trapdoor problem has been investigated by a considerable number of researchers. Engnesser [1] pioneered the experimental studies of trapdoors under normal earth gravity. His tests included strip trapdoors underlying sands of varying heights. Terzaghi [2], Ladanyi and Hoyaux [3], Evan [4] and Tanaka and Sakai [5] reported plane-strain active tests in sand while McNulty [6] reported tests on circular trapdoors with surcharge loads. These experimental studies have shown that the soil load on the trapdoor is substantially lower than the initial geostatic loads when the trapdoor is moved even slightly in the download direction (in the active mode). In granular materials, the amount of load reduction is a function of the overburden depth, the trapdoor size, the friction angle, the granular medium's dilation angle and the relative displacement between the soil and the trapdoor. Stress redistribution or arching occurs when load is transferred to the adjacent stiffer parts of the soil in response to lowering of the trapdoor, with the state of so-called maximum arching being reached as the minimum load on a trapdoor is mobilised.

Centrifuge tests under elevated acceleration levels have also been used to model trapdoor problems. Abdulla and Goodings [7] studied the effects of pre-existing voids in weakly cemented sand and clay. Stone and Wood [8] tested controlled movement of trapdoors in sands and clay. Costa et al [9] studied the presence of presence of pipe inclusions directly

above active trapdoors in sand. The focus of these centrifuge tests was the mechanism of deformation in the soil above the trapdoor and the load on the trapdoor was not measured. Iglesia [10] and Iglesia et al. [11] measured the load on trapdoors in the centrifuge and studied factors affecting the amount of load reduction in plane-strain trapdoors. Dewoolkar et al. [12] carried out centrifuge tests on circular trapdoors underlying sand. Rui et al [13] presented a series of plane-strain centrifuge experiments to study the interaction between multiple trapdoors. Jacobsz [14] studied the evolution patterns of the shear bands in deep trapdoors in the centrifuge to gain insight into the propagation of cavities towards the ground surface, ultimately leading to sinkhole formation.

The scaling challenges to achieve complete similarity between centrifuge models and prototypes of trapdoors in sand have been discussed in detail by Iglesia et al. [15]. A parametric study to investigate the effects of g-level, grain-size, trapdoor width and overburden depth has been conducted. It was found that the particle-size scaling becomes unnecessary when the trapdoor width is greater than 20 times the grain size.

Several theoretical studies on trapdoors have also reported in the literature. Closed form solutions for load reduction of trapdoors were developed by Engesser [1], Terzaghi [2], Bierbaumer [17] and Krynine [18] using limit equilibrium methods. Detailed validation and discussion of the assumptions used in these methods can be found in [11]. Rui et al [19] used limit equilibrium to study the evolution of soil arching which considers interaction between multi-trapdoors. Solutions based on limit analysis have been developed by Davis [20], Gunn [21] and Martin [22] for plane-strain trapdoors in undrained clay and by Smith [23] [24] for shallow trapdoors in sand. Sloan and Assadi [25] used Finite Element Limit Analysis (FELA) to study trapdoors in undrained conditions. In their formulation linear stress (lower bound) and linear velocity (upper bound) triangular finite elements were used to discretize

the soil mass. Every node in the FELA mesh is unique to a particular element so that statically admissible stress (LB) and kinematically admissible velocity discontinuities (UB) can occur along shared edges between adjacent elements. Wang et al. [26] used FELA with adaptive re-meshing to obtain lower bound solutions to the minimum load on trapdoor. Wang et al. [26] also obtained upper bound solutions using a discontinuity layout optimization (DLO) algorithm [27]. The DLO algorithm makes use of mathematical optimization techniques to define a critical layout of slip lines. Finite element (FE) analysis of trapdoors has been carried out by Koutsabeloulis and Griffiths [28] to study the displacement response and minimum load on trapdoors in a range of geometries and soil properties. Tanaka and Sankai [5] back analysed their experimental data using finite element analysis. FE was also performed by Nakai et al. [29] but the focus was on shear bands and the development of slip surfaces. In the theoretical studies mentioned above there is limited discussion on the effect of dilatancy of granular materials on the state of maximum arching, with the exception of Smith [24] who developed limit analysis solutions for shallow trapdoors in non-associative soil.

This paper focuses on evaluating the conditions of maximum arching developing during the lowering of plane-strain active trapdoors in granular materials. The paper presents results of 350 finite element analysis simulations aimed to investigate various factors affecting the maximum arching conditions in active trapdoors, with a particular focus on the effect of soil dilatancy. The paper also presents rigorous upper bound limit analysis solutions which provide a further check on the results obtained using finite element analysis.

2. Methodology

2.1. Finite element analysis

ABAQUS/Explicit finite element software [30] was used to simulate trapdoor experiments. A plane-strain idealisation was adopted for the vertical penetration of the trapdoor experiment. The trapdoor width (B) is taken to be 2.032m, and the width of the soil mass is taken to be 26.4m. These dimensions correspond to the prototype scale for 80g acceleration centrifuge models of trapdoors at carried out at MIT and reported by Iglesia et al. [11]. The geometry and the mesh of the finite element model are shown in Fig. 1. Due to symmetry, only half of the whole model is considered. Only the base of the strongbox is modelled since the strongbox in trapdoor experiments is wide, and the details of the side walls will have negligible effect on the dominating behaviour. In the finite element analyses, a perfectly rigid strongbox is assumed. Roller conditions are assumed at the outer vertical side and the centreline. The vertical faces are constrained from moving in the normal direction. Full fixity boundary conditions are applied to the rigid strongbox. A constraint is imposed such that the motion of the nodes and the surfaces are governed by a single rigid body reference node. The positions of the nodes and the surfaces of the rigid body remain constant throughout the simulation.
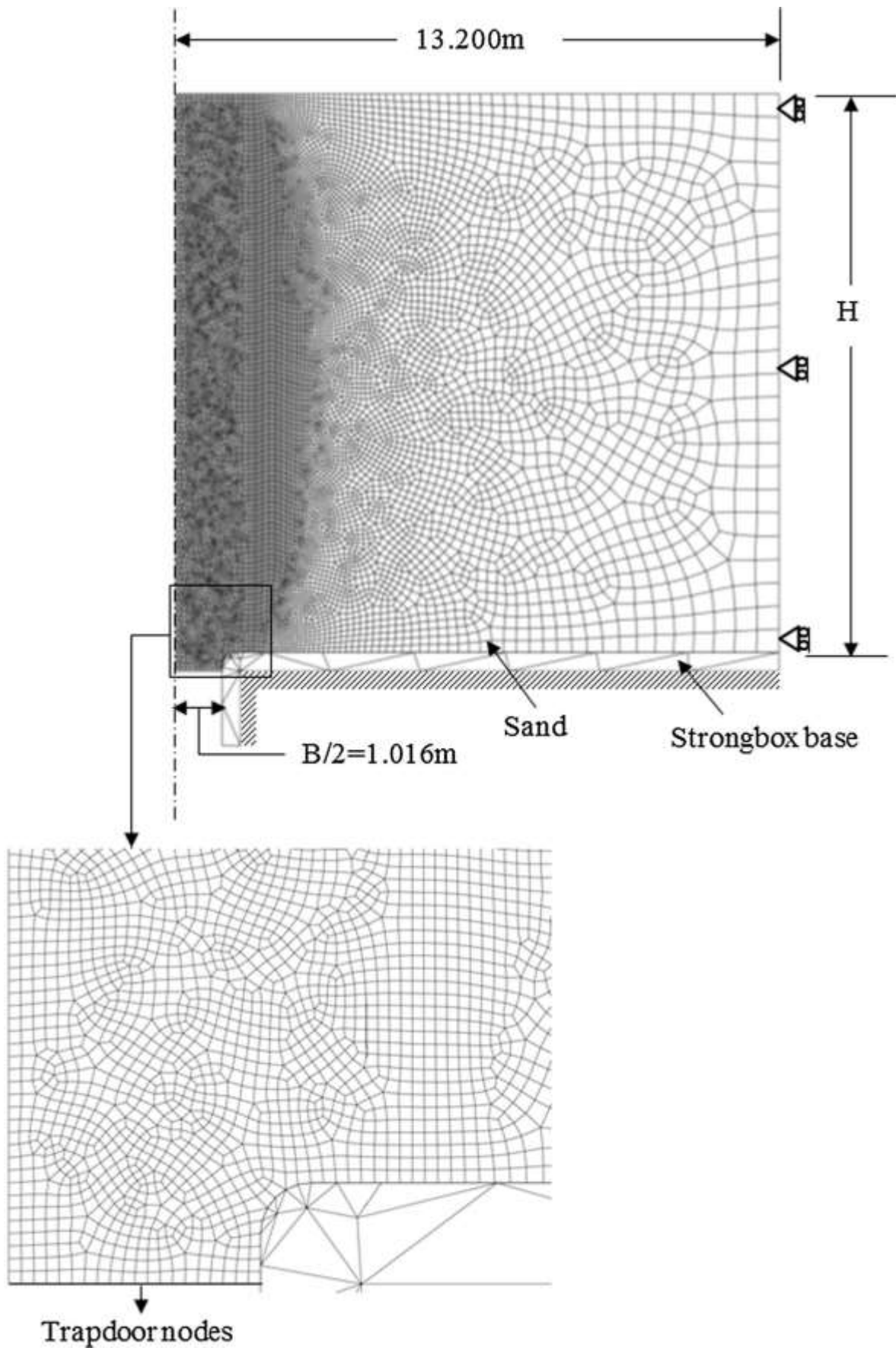
Fig. 1. Finite element mesh.

In typical trapdoor experiments, a piston connected to the trapdoor is lowered at a constant rate and the soil particles flow under the gravity. It would, therefore, be overreaching to assign any particular velocity profile for the soil in the trapdoor zone. Since the interest is not in the flow of the sand in the piston compartment, the trapdoor level is assumed to be lower than the base of the strongbox at the beginning of the analysis by 0.2B and an imposed vertical displacement is applied to the bottom nodes of the sand. The bottom nodes are restricted to move in the vertical direction only. Rounded corners are assumed at the connection between the piston compartment and the strong as shown in Figure 1 to avoid numerical problems. The corners are trimmed with a radius of the fillet equal to 0.1B. This value was selected following preliminary analyses to ensure stability during the large deformation contact analysis.

Bilinear plane-strain quadrilateral, reduced integration, hourglass control elements are used to simulate the granular material. Adaptive re-meshing with the Arbitrary Lagrangian Eulerian algorithm [31] are activated. Since the use of bilinear elements will require the use of dense meshes to achieve an accurate solution in elasto-plastic materials, the finite element mesh is selected to have an element size of B/40 near the trapdoor and size of B/4 at the far boundary. The strongbox is modelled with discrete rigid elements. It should be noted that no high order elements are available in ABAQUS/Explicit with adaptive re-meshing. Small displacement analysis without adaptive re-meshing has shown that, with the adopted mesh geometry and element sizes, the bilinear quadrilateral elements give almost identical results to the built-in six nodded triangular elements.

Explicit solution procedures were used in the finite element analysis. An advantage of the explicit procedure compared to the implicit procedure is the increased ease with which it

resolves complex contact problems. The interaction between the soil and trapdoor is calculated using a frictional interaction, with the sand characterized by a coefficient of friction μ of 0.2. This value is based on the back analysis of centrifuge tests of trapdoor in sands carried out the University of Pretoria. Ideally, the coefficient of friction should not be a constant and it should depend on the relative motion between the surfaces in contact the angle of friction of sand. However, using a constant coefficient of friction could represent a reasonable approximation since the focus here on the maximum arching in the sand above the trapdoors. This contact algorithm incorporates a finite-sliding formulation, allowing for arbitrary motion of the surface.

The analyses were carried out into two steps. In the first step geostatic stress initial conditions are applied with zero movement of the trapdoor. A gravity load of 10 m/s^2 is applied to the whole model. The value of 10 m/s^2 represents a reasonable approximation for gravity. In the second step, a vertical displacement-rate of 0.013 m/s is imposed on the trapdoor nodes. The explicit solution method represents a true dynamic procedure which was originally developed to model high-speed impact events in problems in which inertia plays a dominant role in the solution. In the solution procedure out-of-balance forces propagate between neighbouring elements as stress waves, while solving for a state of dynamic equilibrium. The minimum stable time increment is normally small so that most problems require a large number of increments. Applying the explicit dynamic procedure to quasi-static problems requires certain special considerations. ABAQUS includes a built-in smooth step amplitude curve that automatically creates smooth velocity amplitudes, where the displacement rate increases from zero to 0.013 m/s in 1 second. Using this type of smooth step amplitude allows performing a quasi-static analysis, avoiding the generation of waves due to discontinuity in the rate of applied displacement.

The soil is taken to be linear elastic perfectly plastic. The Mohr-Column yield criterion is adopted in the analyses. Unless otherwise stated, Young Modulus (E) is taken to be 100 MN/m^2 and the Poisson's ratio is taken to be 0.4. The soil mass is assumed to have a density of 1600 kg/m^3.

2.2. Upper bound rigid-block analysis

This study also considered a rigid-block mechanism to model the upper bound stability of trapdoors. This provided a further verification of the solutions from the finite element analysis and was developed to visualise the deformation mechanisms associated with minimum loads in trapdoors. The triple rigid-block mechanism considered is shown in Fig. 2. This mechanism could be regarded as an extension to Gunn's mechanism [21] which was developed for trapdoors in undrained clay. In Fig. 2, A_i refers to the area of rigid-block I, v_i refers to the kinematically admissible velocity of the rigid block, v_{ij} to the velocity jump along the discontinuity between blocks i and j, L_{ij} to the length of segments between blocks i and j, while α, β, and η represent the unknown angular parameters defining the rigid block mechanism geometry. The soil mass is assumed to be governed by the Mohr–Coulomb failure criterion and an associated flow rule are assumed so that the dilation angle ψ is taken to be equal to the friction angle ϕ. The compatible velocities v_i and v_{ij} can be calculated from the hodograph shown at the right side of the block mechanism. The upper bound solutions derived from the mechanism is given by:

$$-\sigma_{V,trapdoor} \leq \frac{c \times cos\phi \times (l_{10} \times v_1 + l_{20} \times v_2 + l_{21} \times v_{21} + l_{32} \times v_{32}) - \gamma \times (A_1 \times v_1 + A_3 \times v_3 + A_2 \times v_2 \times sin(\beta - \phi))}{(B / 2 \times v_3)}$$

(1)

where $\sigma_{V,trapdoor}$ is the average vertical stress at the trapdoor level, B is the width of the trapdoor, γ is the unit weight of soil and c is the soil cohesion. Since the focus here is active trapdoors in sand, the soil is taken to be cohesionless ($c=0$).
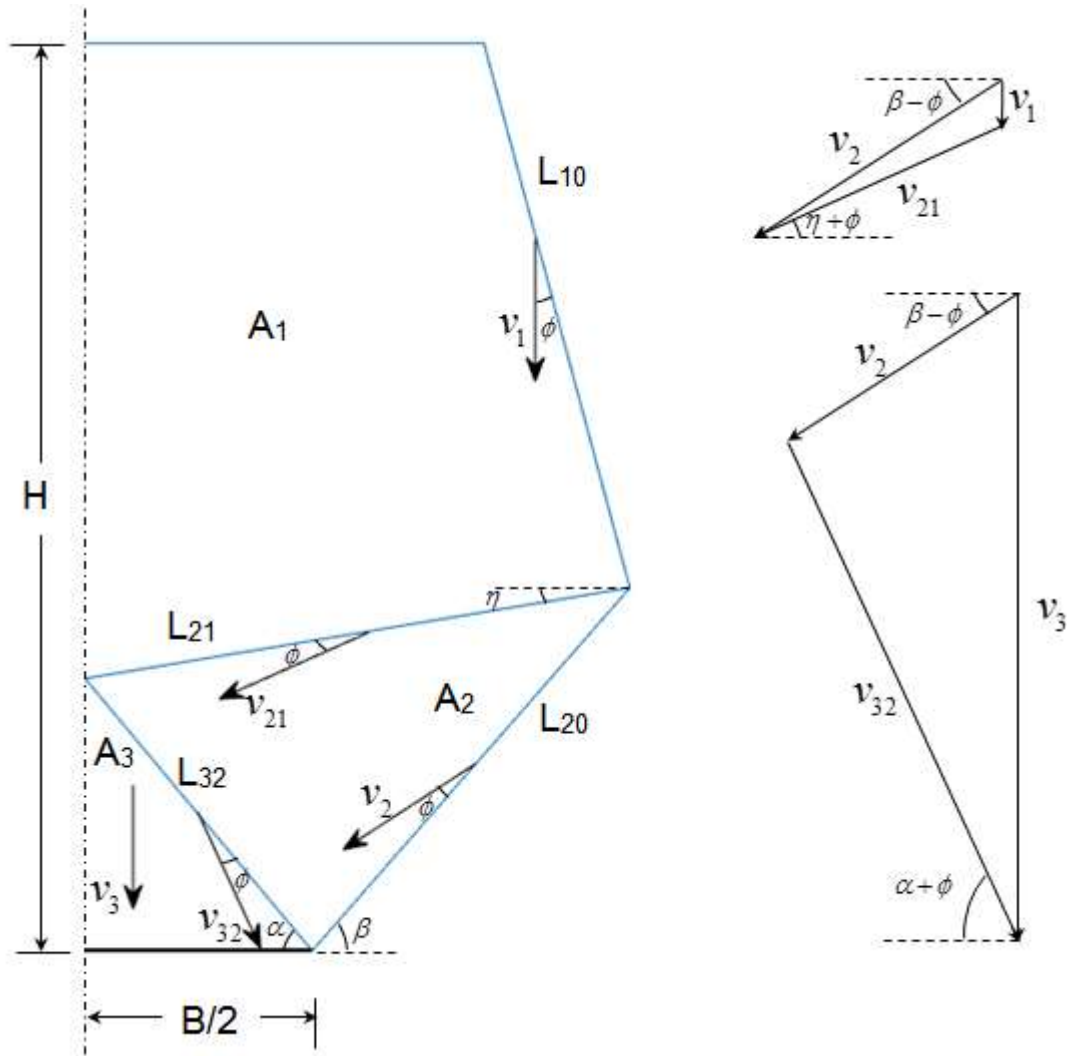

Figure 2: Upper bound rigid block mechanism

The state of maximum arching (or minimum load on trapdoor) is often expressed in terms of the load ratio (P/P$_o$), where P represents the average vertical load on a trapdoor and P$_o$ refers to the free field vertical load. Therefore, the load ratio (P/P$_o$) can be expressed as:

$$\frac{P}{P_o} = \frac{\sigma_{V,trapdoor}}{\gamma H} \tag{2}$$

where H is the height of the soil mass above the trapdoor.

The minimum upper bound solution is obtained by optimising the geometry of the rigid block mechanism using the MATLAB Optimization Toolbox. The geometry of rigid blocks is allowed to vary subject to the constraint that the areas of the rigid blocks and lengths of the discontinuity lines remain positive.

3. Results and discussion

3.1. Maximum arching

Fig 3 shows the minimum load ratio (P/P_o) in active trapdoors at different normalised depths (H/B) obtained from finite element analysis, the upper bound rigid block mechanism of Fig 2. The results are shown for different friction angles for associative soil ($\psi=\phi$). The finite element analysis and the upper bound solutions are compared with the limit analysis solutions of Wang et al [26]. Wang et al. [26] used the discontinuity layout optimization (DLO) algorithm [27] to obtain an upper bound (UB) and finite element limit analysis FELA [32] with adaptive re-meshing to obtain lower bound solutions. Figure 3 shows that the finite element analysis is in good agreement with the limit analysis of Wang et al. The simple upper bound rigid block mechanism solution is consistent with the advanced DLO-UB, although it slightly overestimates the maximum arching in trapdoor for deeper trapdoors (H/B> 5) at small friction angles. It should be noted that the advanced computational DLO-UB does not require a priori assumptions regarding the kinematics or location of a collapse state. While the number of rigid blocks in the mechanism of Figure 2 is limited to three, there is no such limit in DLO-UB in Wang el [26] and the number of slip lines is optimised using 2000 nodes.
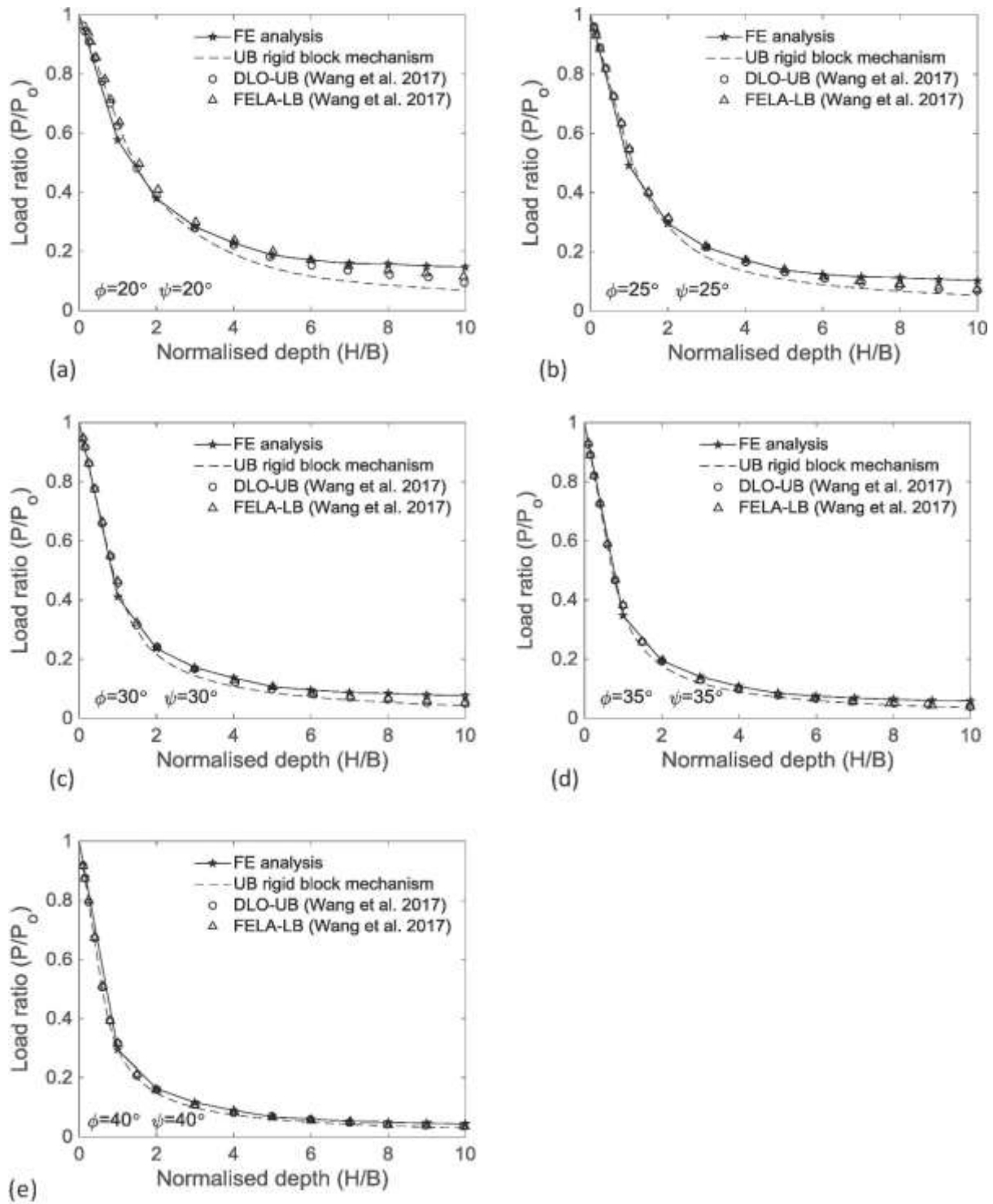
Fig. 3. Mobilised trapdoor loads at conditions of maximum arching on trapdoors in associative MC soil (): (a) $\phi = 20°$ (b) $\phi = 25°$ (c) $\phi = 30°$ (d) $\phi = 35°$ (e) $\phi = 40°$.
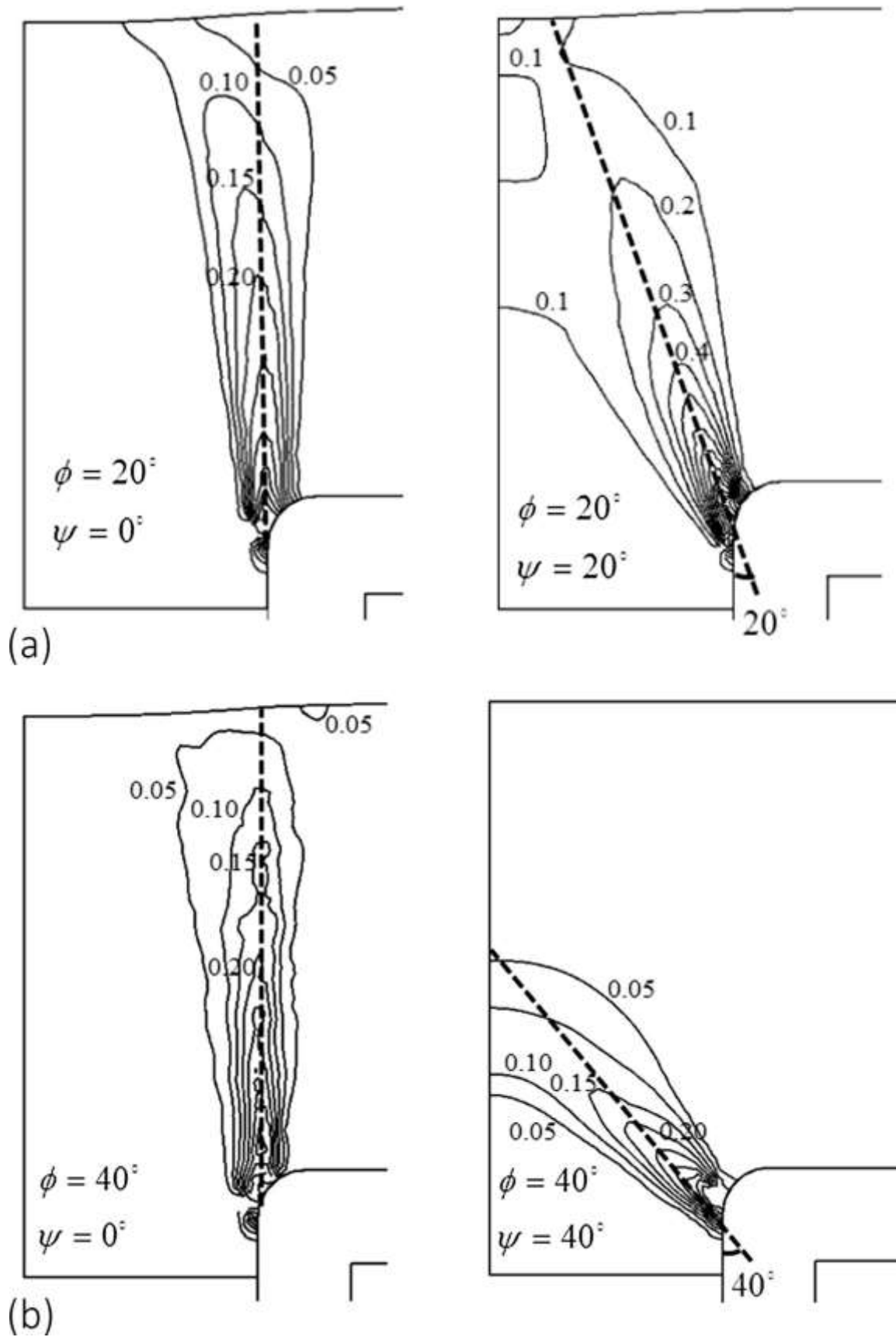
Fig. 4. Contours of plastic engineering shear strain (shown at equal intervals) above a shallow trapdoor (H/B = 1) at conditions of maximum arching: (a) $\phi = 20°$ (b) $\phi = 40°$.

Figure 4 shows the pattern of the plastic engineering shear strain contours at maximum arching at a shallow trapdoor with a normalised depth (H/B=1). The strain contours are shown for two angles of friction: ϕ=20° and ϕ=40°. For each angle of friction, the shear strain contours are plotted for two extreme cases of dilatancy: $\psi=\phi$ (associative MC) and ψ=0°. The plastic engineering shear strain ε_s^p is defined as:

$$\varepsilon_s^p = \left| \varepsilon_1^p - \varepsilon_3^p \right| \tag{3}$$

where ε_1^p and ε_3^p are the major and the minor plastic principal strain, respectively.

Figure 4 shows that the shear bands characterised by an inclination to the vertical approximately equal to the dilation angle with the exception to areas near the free surface and the centreline where the inclination is greater than the dilation angle. It should be remembered that in reality the dilation angle depends on stress level and varies during the plastic deformation preceding failure and that it tends towards zero at the critical state (see [33] for example). However, a constant rate of dilation is often assumed in practice in the absence of suitable laboratory or field data.

Figure 5 shows that plastic engineering shear strain contours at a deep trapdoor (H/B=10) at conditions of maximum arching. The contours are shown for ϕ=40° for four dilation angles ψ=0°, ϕ/4, ϕ/2 and ϕ. The dotted lines have inclination from the vertical approximately equal to the angle of dilation. Comparing Figure 5 with Figure 4, it can be concluded that the deformation mechanism and shear band patterns in deep trapdoors are different from shallow trapdoors. At maximum arching in a deep trapdoor, the deformation mechanism is localised and even at zero dilation angle the shear bands do not propagate to the soil surface. The shear bands initiate from the edges of the trapdoor at an inclination equivalent to the dilation angle;

however, the bands curve inwards towards the centerline. In non-associative soils, more than one shear band or (slip surface) can be observed.
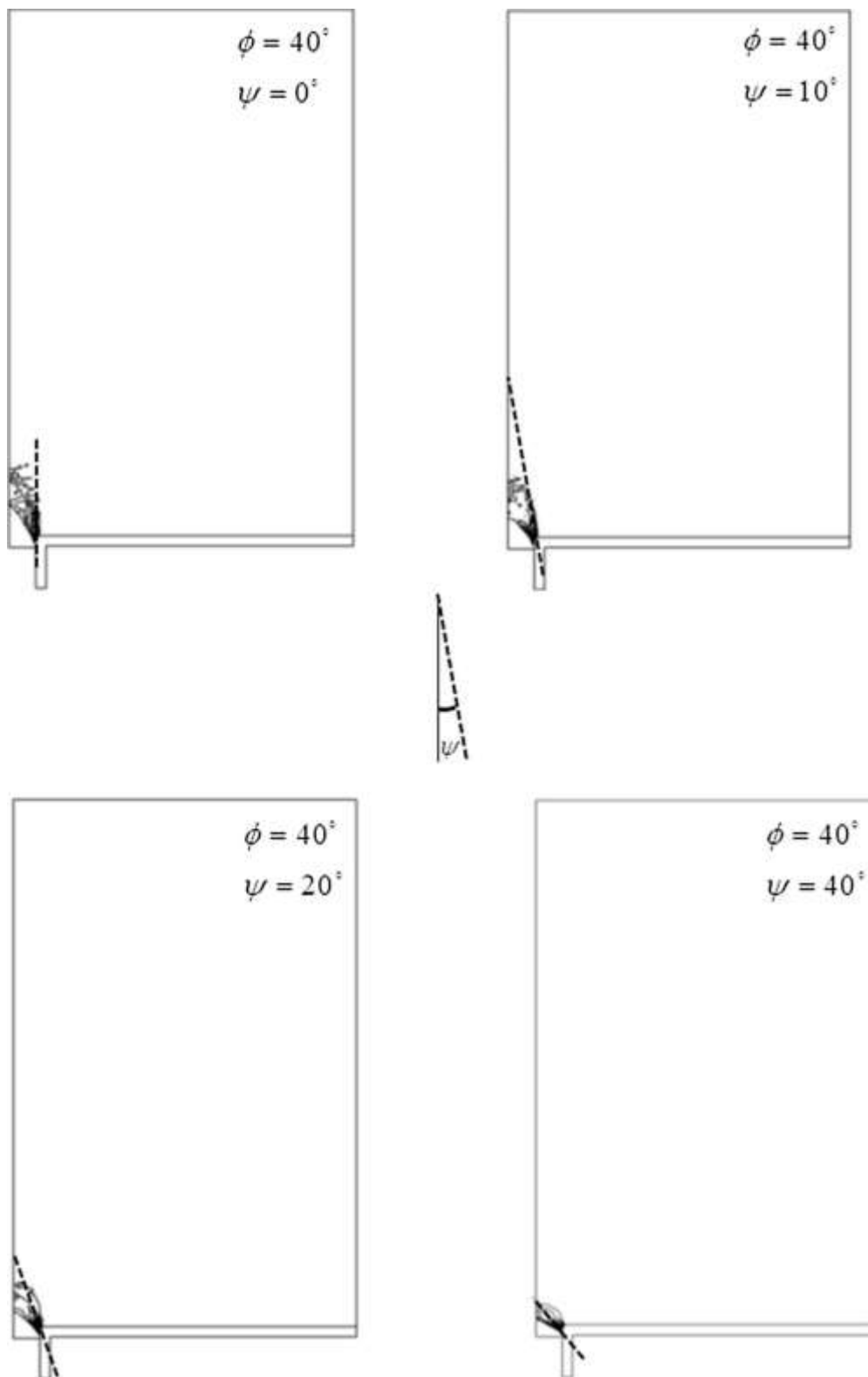
$\phi = 40°$
$\psi = 0°$

$\phi = 40°$
$\psi = 10°$

$\phi = 40°$
$\psi = 20°$

$\phi = 40°$
$\psi = 40°$

Fig. 5. Contours of plastic engineering shear strain above a deep trapdoor (H/B = 10) at conditions of maximum arching.

$\phi = 20°$
$\psi = \phi$
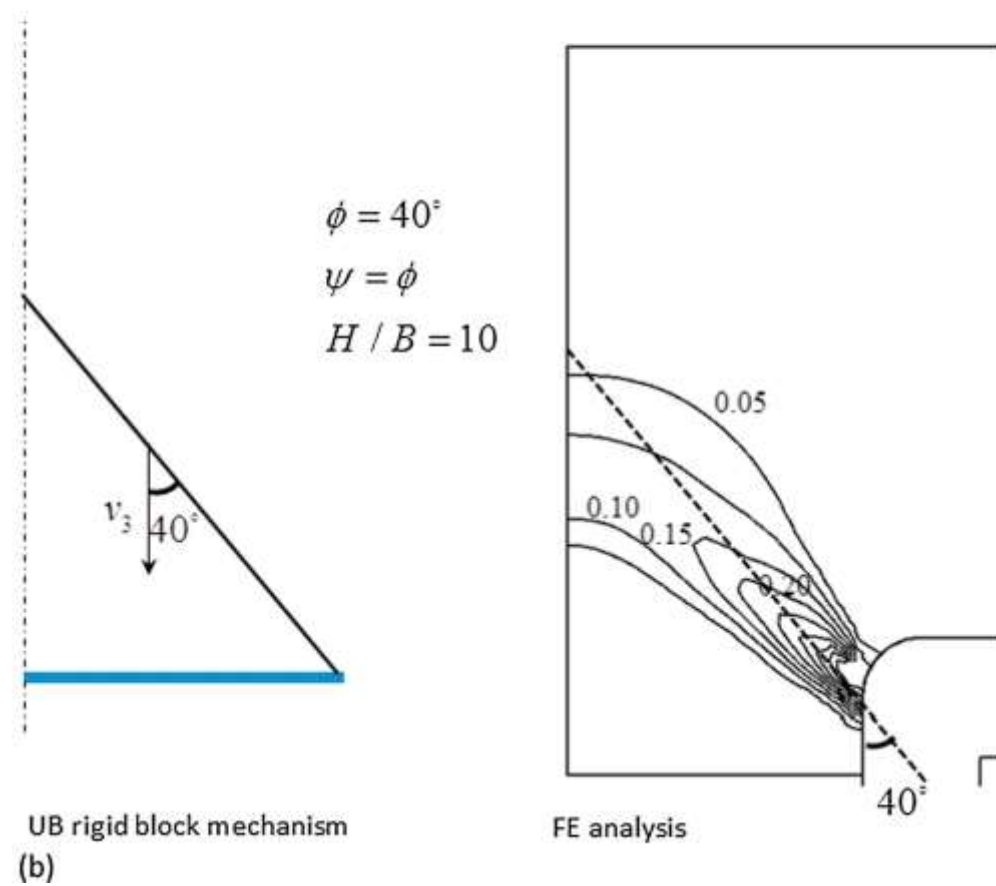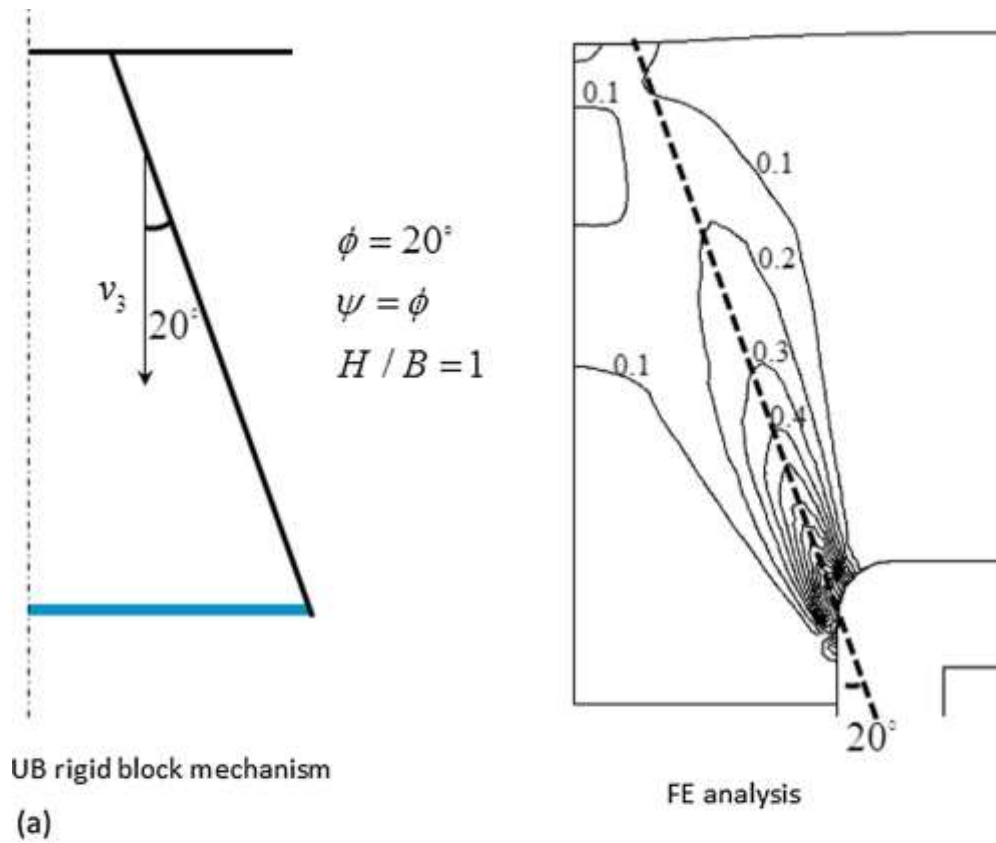$H / B = 1$

UB rigid block mechanism

(a)

FE analysis

$\phi = 40°$
$\psi = \phi$
$H / B = 10$

UB rigid block mechanism

(b)

FE analysis

Fig. 6. Contours of plastic engineering shear strain (shown at equal intervals) in (a) shallow trapdoor H/B = 1 (b) deep trapdoor H/B = 10.

Figure 6 shows that the rigid block mechanism of Figure 2 is capable of replicating different modes of plastic deformation mechanism trapdoors. It should be noted that the finite element method is a continuum approach in which the locations of the slip lines (the dotted lines) can be inferred from plastic strain shear bands. For $\phi=20°$ and H/B=1, the optimum upper bound solution obtained with angular parameters $\alpha=32.4°$, $\beta=110°$ and $\eta= 30.0°$. At these angular parameters, the velocity jumps along the discontinuities between the rigid blocks vanish ($v_{21} = v_{32}=0$) and the mechanism collapses to a single rigid block as shown in Figure 6a. For a deep trapdoor H/B=10 and for $\phi=40°$, the optimum geometry is achieved with $\alpha=50°$, $\beta= 69.2°$ and $\eta= 65.1°$. At this geometry, the velocities v_1 and v_2 vanish and the mechanism reduces to a single slip line with $v_{32} = v_3$ as shown in Figure 6b. The associative flow rule finite element results for H/B=10 and $\phi=40°$ show a slip curve rather than a line with an initial inclination from the vertical equal to the dilation angle and an increasing inclination towards the centreline. This might explain the slight discrepancies in predicting the maximum arching conditions between the finite element method and the rigid block mechanism.

3.2. Effect of soil dilatancy

Figure 7 shows the minimum load at conditions of maximum arching (or minimum load on trapdoor), expressed in terms of the load ratio (P/P$_o$) plotted against normalised depth (H/B). The effect of the dilatancy was investigated for friction angle values between 20° and 40° at 5° intervals. For each angle of friction, the results are shown for four values of dilation angles equal to 0°, ϕ/4, ϕ/2 and ϕ. Figure 7 shows that the effect of dilatancy is more significant in a shallow trapdoor and reduces with the increase of overburden soil. For $\phi=40°$, for example, in the case of H/B=1, the load ratio with zero dilation is about 34% higher than that calculated assuming associative flow rule, while the difference reduces to about 14% at a normalised depth H/B=10.
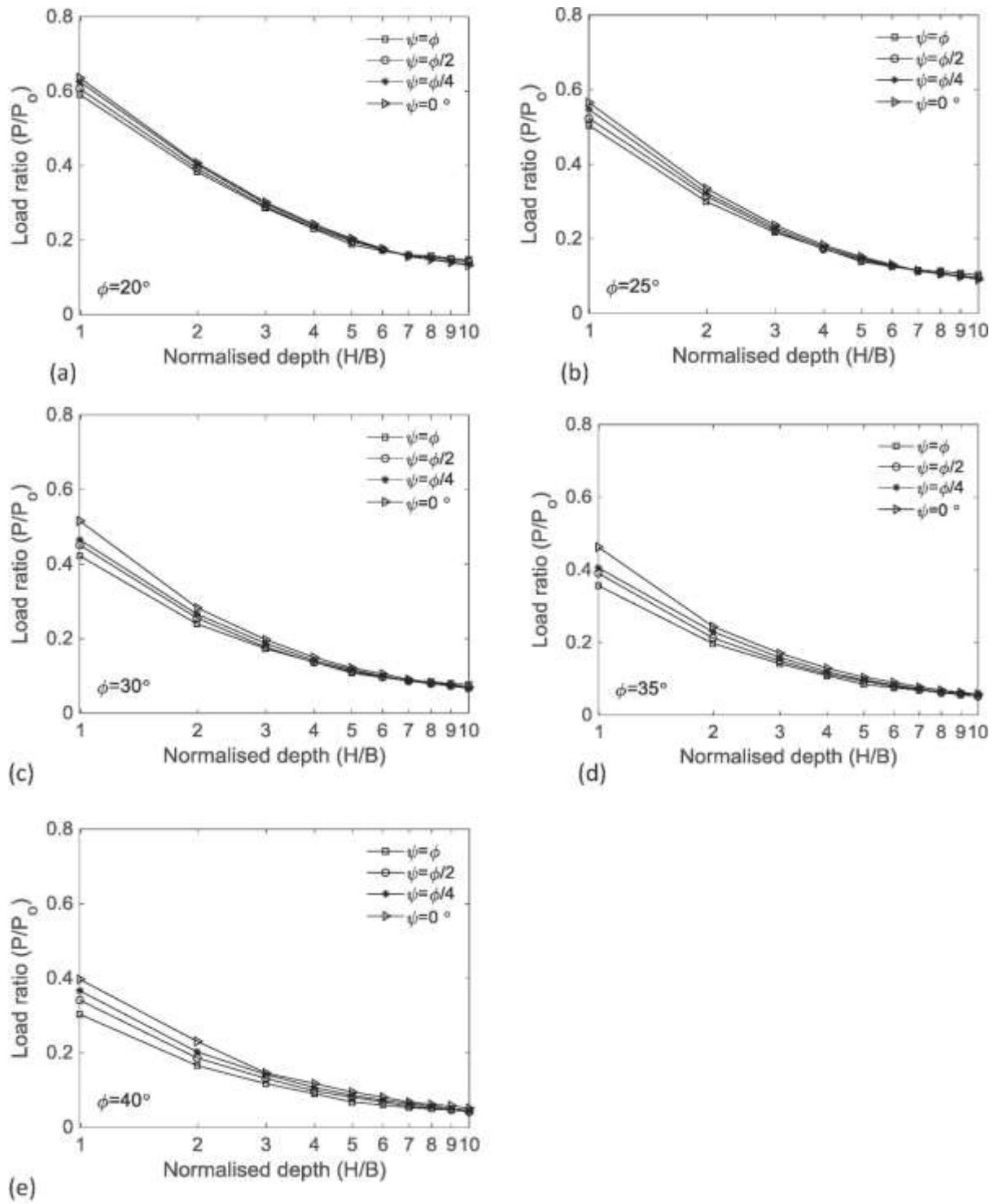
Fig. 7. Effect of soil dilatancy on mobilised trapdoor load at conditions of maximum arching: (a) $\phi = 20°$ (b) $\phi = 25°$ (c) $\phi = 30°$ (d) $\phi = 35°$ (e) $\phi = 40°$.

Smith [24] developed equilibrium limiting stress fields and compatible velocity fields for a shallow anchor/trapdoor problem in non-associative cohesionless soils. The limiting loads are expressed as:

$$\frac{P}{\gamma HB} = 1 \mp \frac{H}{B} \Upsilon \qquad (4)$$

where the sign depends on whether the displacement is active (-) or passive (+) and the non-dimensional function Υ, in Smith's analysis [24], is evaluated entirely from the angle of friction ϕ and the dilation angle ψ.

In this paper Υ is back-calculated from the results of the upper bound rigid block mechanism and finite element method. In active trapdoors Equation 4 can be re-written as:

$$\Upsilon = \left(1 - \frac{P}{P_o}\right) \Big/ \left(\frac{H}{B}\right) \qquad (5)$$

Figure 8a plots the value of Υ back-calculated from optimum load ratio (P/P_o) obtained from the rigid block mechanism of Figure 2 assuming the associative flow rule. The soil is taken to have self-weight and there is no surface load. The results are plotted against the normalised depth H/B. It can be seen from these results that Υ in associative soil cannot be evaluated entirely from ϕ (and ψ) unless the trapdoor depth is less than 0.6B in case of ϕ=40° and 1.2 B in case ϕ=20°. At these shallow depths, Υ becomes equal to $\tan\phi$ in associative soils as shown in Figure 8b. Beyond these shallow depths (0.6-1.2B), Υ varies with the height of the soil above the trapdoor.
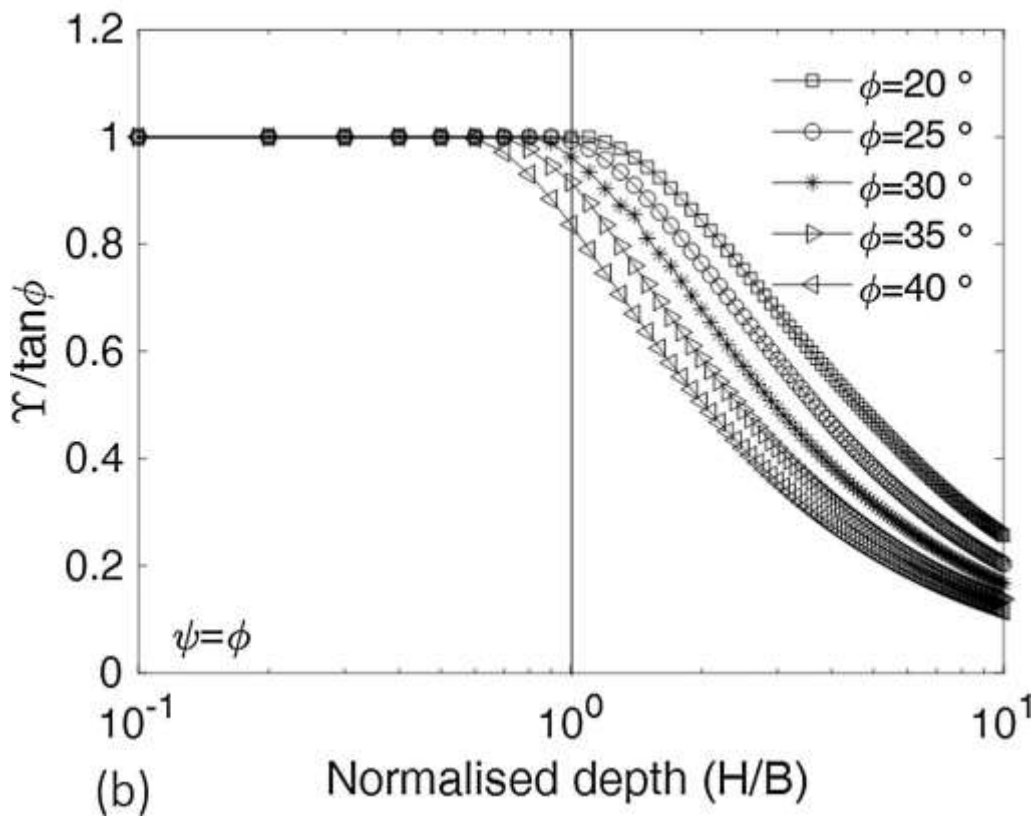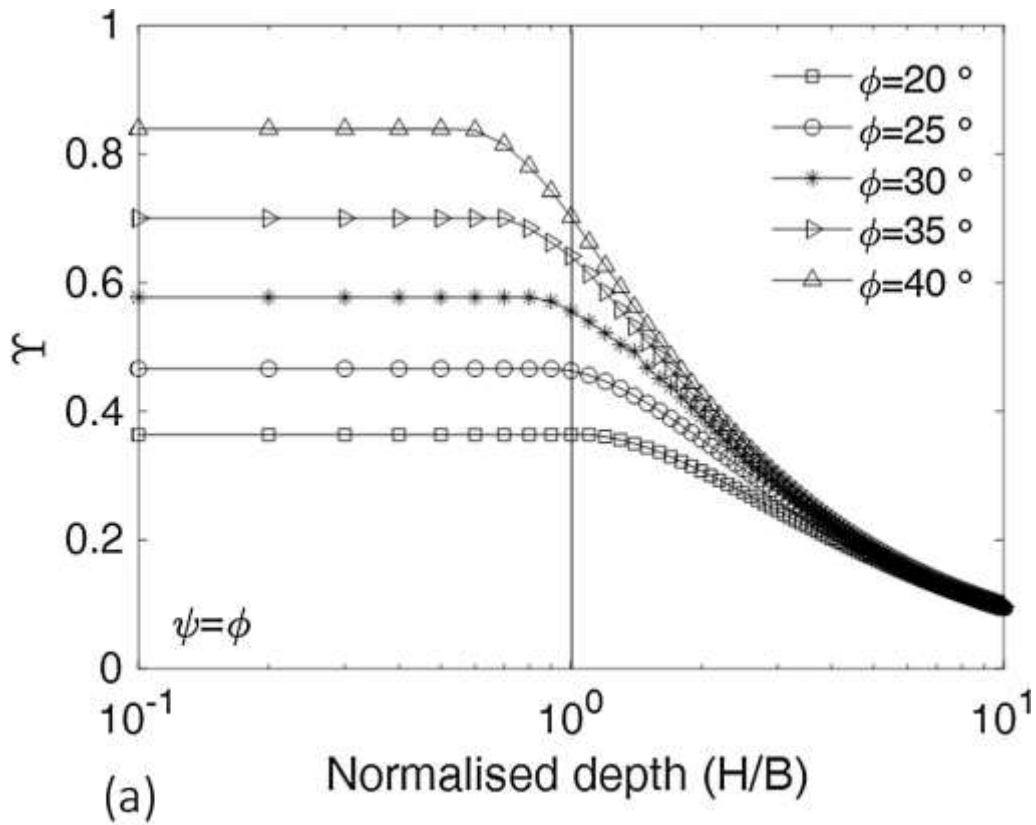
Fig. 8. Variation of value of back calculated from the upper bound rigid block mechanism for an active trapdoor underlying an associative cohesionless soil (a) vs H/B (b) vs H/B.
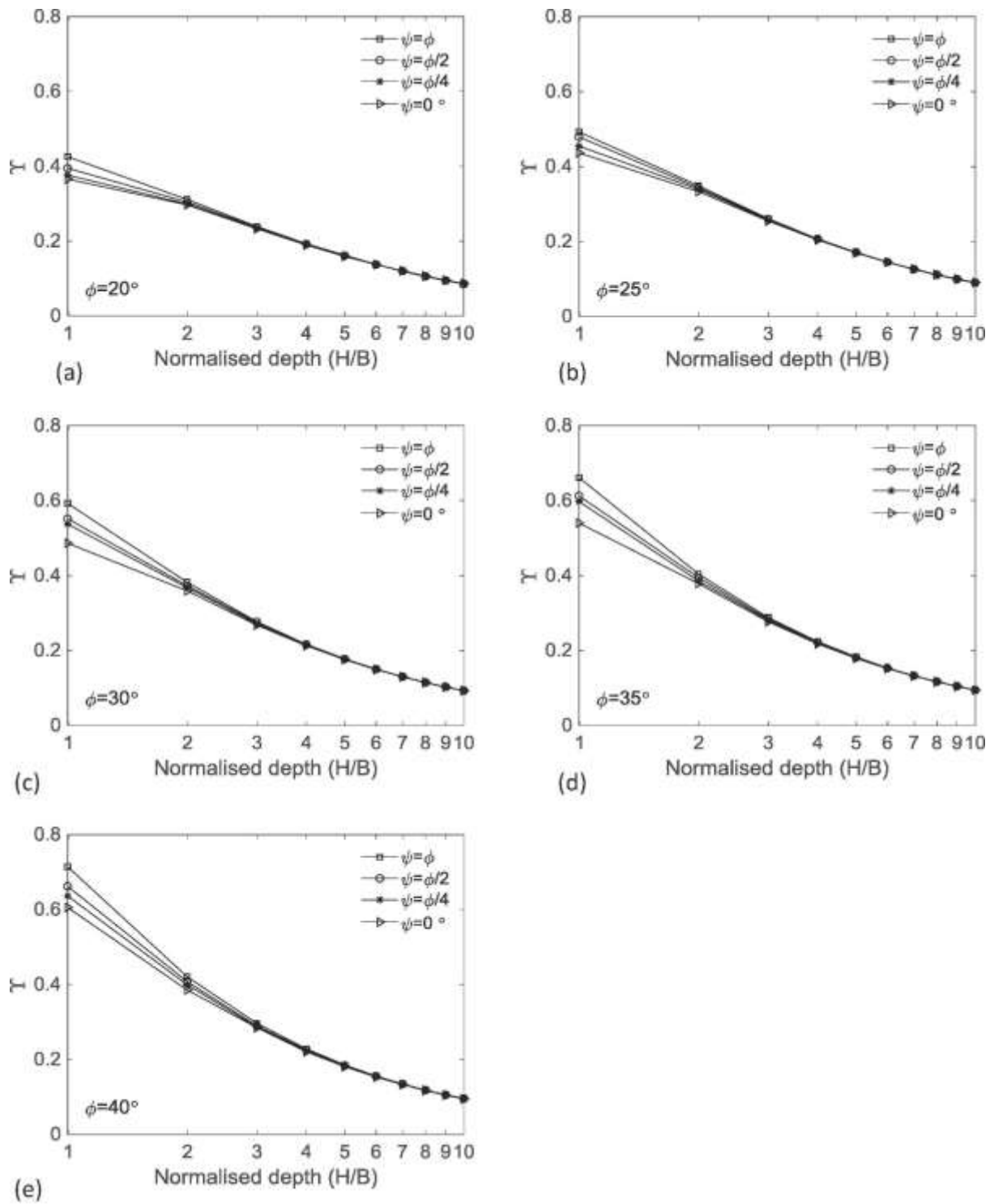
Fig. 9. Variation of the value of back calculated from finite element analysis for an active trapdoor underlying an associative and nonassociative cohesionless soils: (a) $\phi = 20°$ (b) $\phi = 25°$ (c) $\phi = 30°$ (d) $\phi = 35°$ (e) $\phi = 40°$.

Figure 9 shows the variation of the value of Υ back calculated from finite element analysis for an active trapdoor underlying associative and non-associative cohesionless soils. For

ϕ=40 °, for example, in the case of H/B=1, Υ in non-dilating soil is about 13.5% lower than that calculated assuming associative flow rule, while the difference reduces to about 0.8% at H/B=10. It can be concluded from the figure that effect of the angle of dilation on the value of Υ is insignificant for H/B>3 (the differences are less than 3%) and Υ can be approximated as a function of ϕ and H/B at the condition of maximum arching.
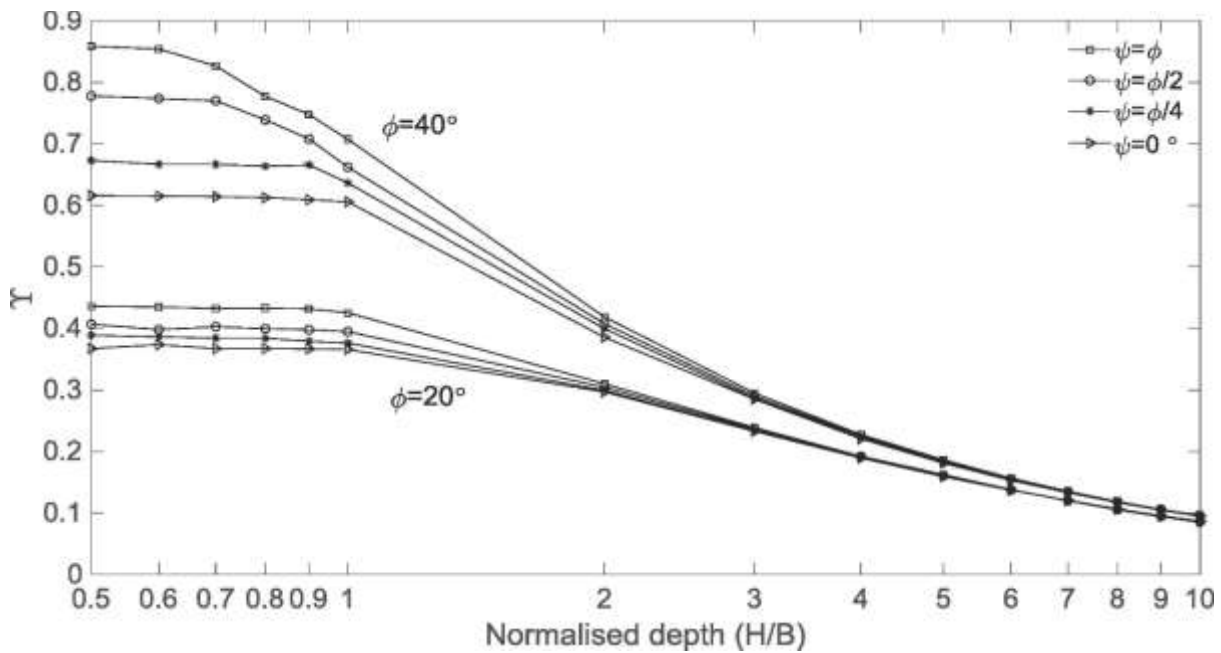

Fig. 10. Variation of the value of back calculated from the FE analysis for an active trapdoor for a wide range of normalised depths.

Figure 10 shows the finite element results for non-dimensional dimensional function Υ plotted for a wide range of normalised depth H/B for for ϕ=20° and ϕ=40°. These results are consistent of the results of rigid-block mechanism shown in Figure 8. At very shallow depths H/B<1, Υ becomes independent of normalized depths. Therefore, direct comparison with the solution developed by Smith [24] for Υ is only possible at very shallow normalised depths. It might be possible to compare the two methods at H/B=0.5 for ϕ=20° and 40° (see Figure 8 and Figure 10). Smith analysis gives values of Υ between 0.363 and 0.366 for ϕ=20° and

between 0.616 and 0.858 for ϕ=40°(estimated from the graph in his paper), while the FE gives a range of 0.374-0.433 for ϕ=20° and 0.697-0.841 for ϕ=40°.

3.3. Approximate analysis for non-associative soils

In soils with high friction angles, the use of an associated flow rule predicts unrealistically large amounts of dilation during shear failure which raise questions about the validity of limit load estimates determined from the bound theorems. Davis [20] reported that the choice of the flow rule will not have a significant influence on limit loads for frictional materials provided that the problem is not statically indeterminate. In the absence of strain-softening, the collapse load for a statically determinate mechanism will not be affected by non-associativity. For an examination of the failure behaviour on slip-lines for a non-associated Mohr– Coulomb material, Davis [20] determined that the shear stress τ and normal stress σ_n can be related by:

$$\tau = c* + \sigma_n \tan\phi*$$

(6)

where $c*$ and $\phi*$ are 'reduced' strength parameters, defined as:

$$c* = c\frac{\cos\psi\cos\phi}{1-\sin\psi\sin\phi}$$
$$\tan\phi* = \tan\phi\frac{\cos\psi\cos\phi}{1-\sin\psi\sin\phi}$$

(7)

Drescher and Detournay [34] showed that the limit load determined from a rigid block mechanism using the associative flow rule using Davis' discontinuity strengths $c*$ and $\phi*$, defined by equations (7), provides an upper bound on the true limit load for non-associated materials with parameters (c, ϕ, ψ). The use of Davis's reduced strengths could provide a

practical way for handling non-associated flow in limit analysis. The trapdoor problem is a statically indeterminate problem as the horizontal stresses are not constrained to a single value at collapse [24].
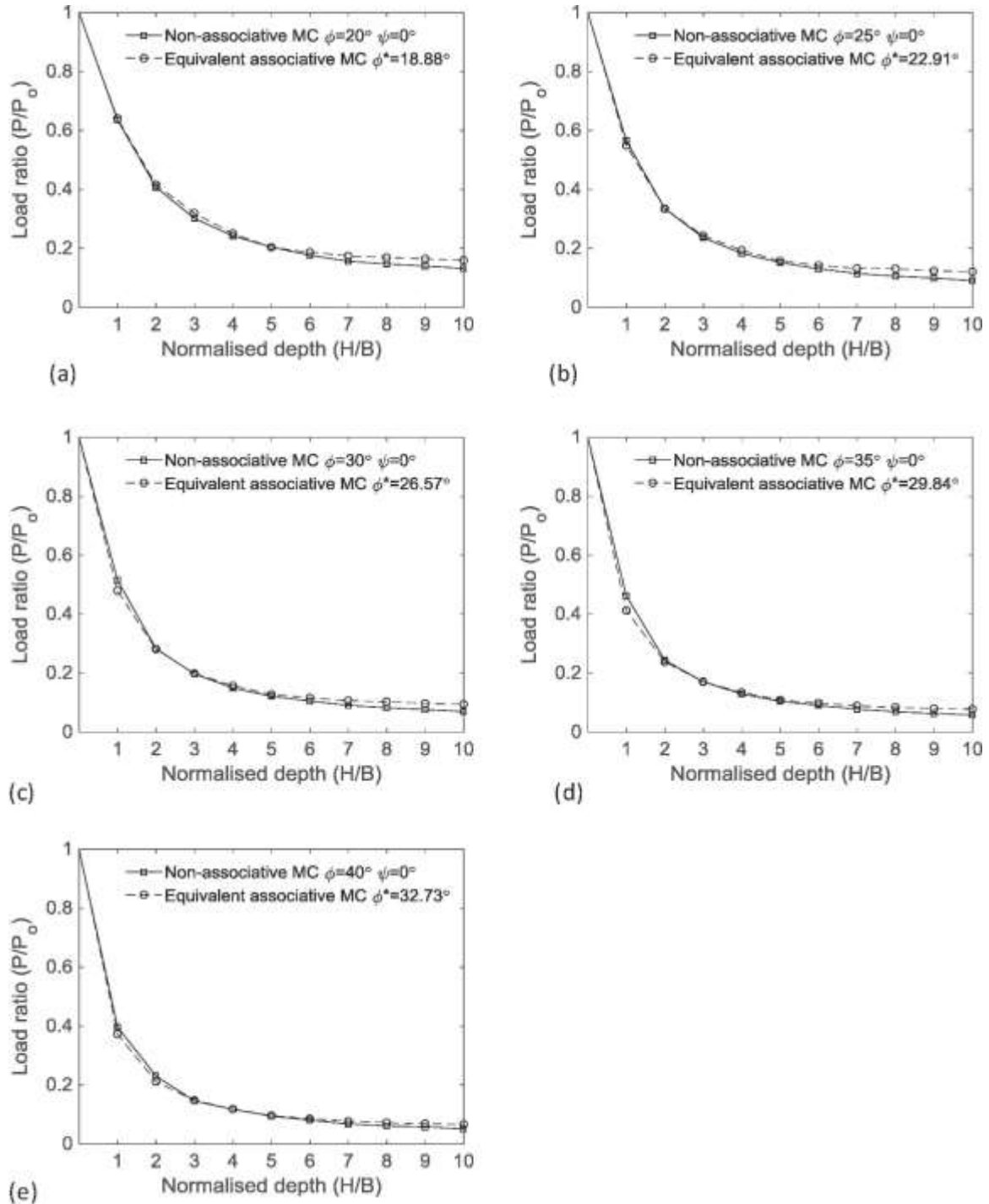

Fig. 11. Comparison between non-associative MC model and associative MC with reduced strength parameters: (a) $\phi = 20°$ (b) $\phi = 25°$ (c) $\phi = 30°$ (d) $\phi = 35°$ (e) $\phi = 40°$.

The validity of the approximate model given by equation 7 in active trapdoors was investigated. Figure 11 compares the results obtained using an equivalent associative Mohr Column model with a reduced angle of friction ϕ^* and those obtained with ϕ and a dilation angle $\psi=0°$. Figure 11 shows that the use of an equivalent associative model with reduced friction angle generally corresponds well with the load ratio from the non-associative model based on actual soil strength parameters, but that it tends to overestimate somewhat. The discrepancy between the two models increases with the increase of depth of the trapdoor. In the case of H/B=10, $\phi=20°$ and $\psi=0$ °, for example, the discrepancy is about 21%.

4. Limitations

The finite element results reported in this paper is obtained by taking the soil to be a linear elastic perfectly plastic material. Mohr-Column yield criterion is adopted with a constant value for the dilation angle. The analyses reported above are carrying out with Young Modulus (E) of 100 MN/m^2 and the Poisson's ratio v of 0.4. The selected values for the elastic parameters might affect the transition mechanisms and the displacements (and the magnitude of the strains) in the soil mass, these parameters would not affect significantly the maximum arching condition (the maximum load reductions in the trapdoors. Figure 12(a) shows results of parametric analyses for a trapdoor with a normalised depth H/B=5 and associated soil with $\phi=30°$ for values of Young Modulus (E) ranges between 50 and 200 MN/m^2 while Figure 12(b) compares the results of load-reduction versus trapdoor displacement for Poisson's ratio (v) 0.4 and 0.2. This figure shows that the variation in the maximum arching results is less than 5%.
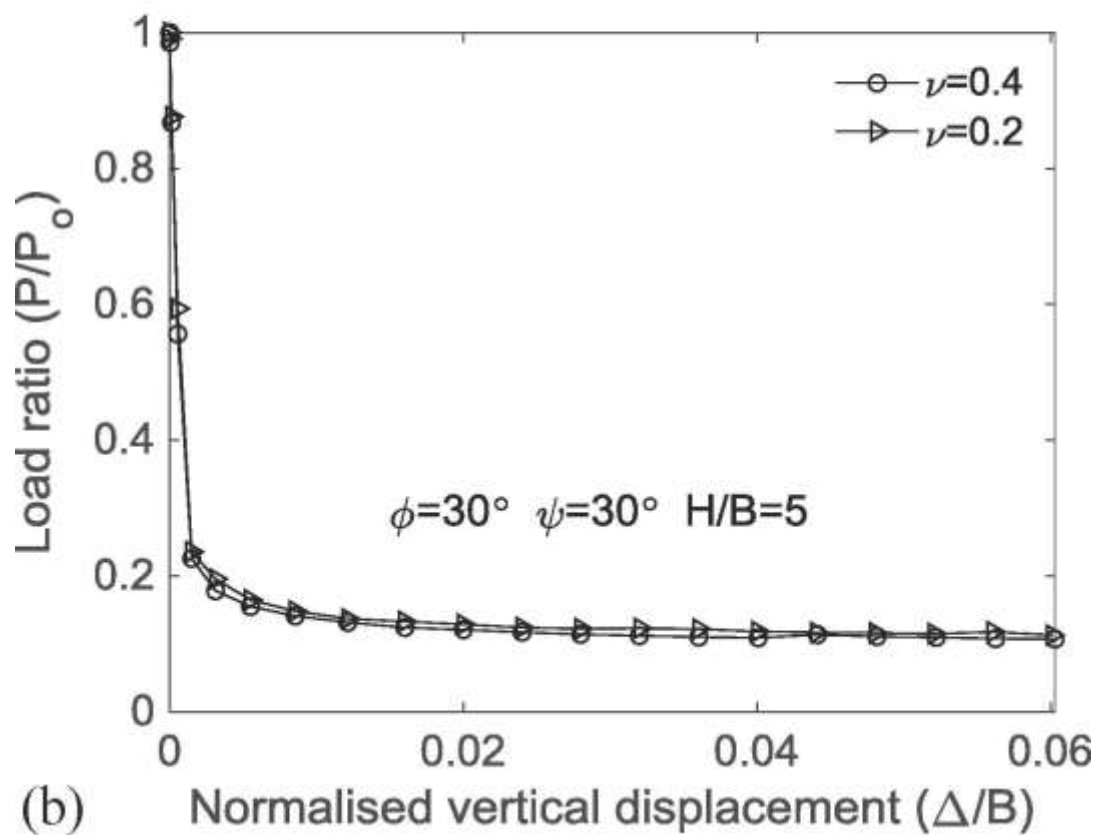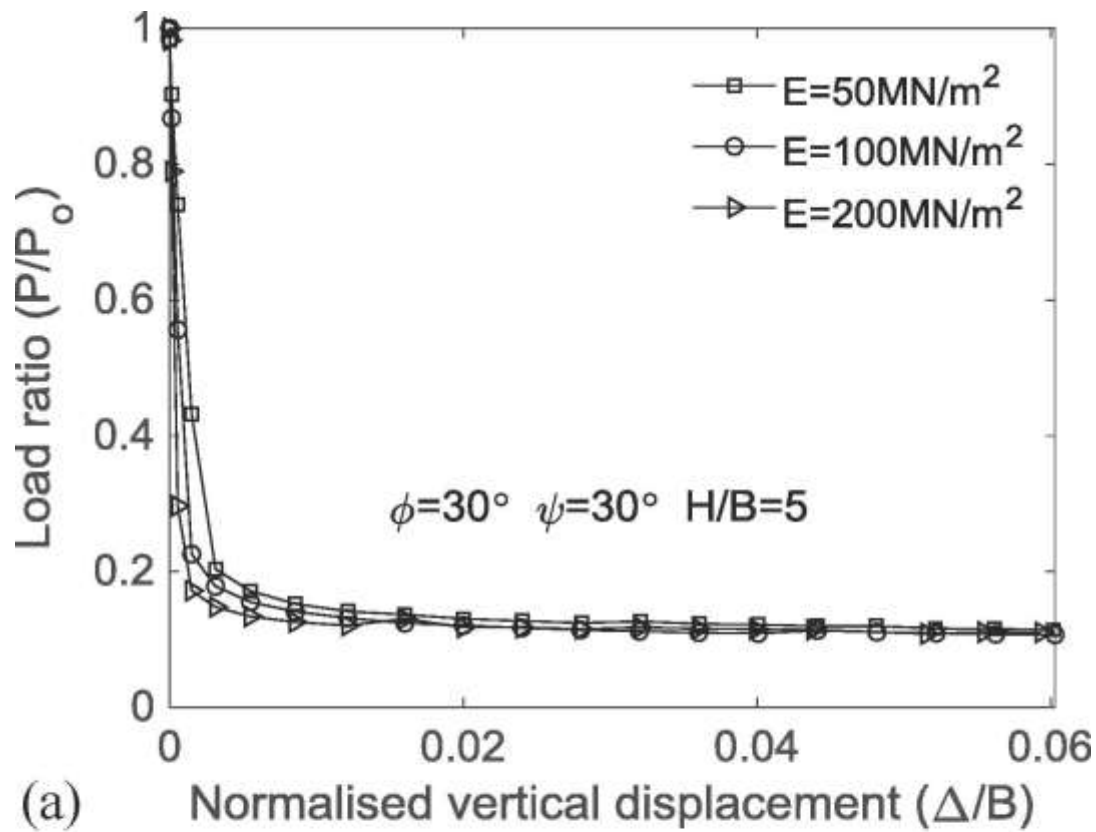
Fig. **12**. Effect of elastic soil parameters on maximum arching (a) Young Modulus (b) Poisson's ratio.

In real sand, the soil stiffness is not constant as it depends on the stress and strain levels. Furthermore, the dilation depends on the plastic strains and it vanishes in the critical state.

However, it should be emphasised that the focus of this paper is the condition of maximum arching above trapdoors in sands where Mohr-Column model could represent a simple and useful tool to shed the light into this complicated phenomenon.

5. Conclusions

The classical trapdoor problem provides a useful tool to understand the stress distribution around a variety of geotechnical structures. The static indeterminacy in trapdoor problems provides an example by which the non-associative and associative solutions can differ. The finite element method presents a viable means of evaluating these types of problems. Explicit finite element solution procedures with the ALE algorithm have been used to investigate the trapdoor mechanism and conditions of maximum arching, with a particular focus on the effect of soil dilatancy. The soil was modelled using the Mohr Column failure criterion with both associative and non-associative flow rules. The associative model shows excellent agreement with previously published computational limit analysis solutions.

A simple rigid-block mechanism for trapdoors in cohesionless soil has been developed for comparison with finite element results and to serve as a practical tool for geotechnical practitioners. Comparison of upper bound solutions obtained from the rigid-block analyses with solutions of the finite element and numerical limit analyses shows consistent results.

The finite element results show that the load ratio with zero dilation can be about 34% higher than that calculated assuming the associative flow rule in a shallow trapdoor while the

difference reduces with the normalised depth. The finite element analysis shows that using the MC model with the associative flow rule and Davis' reduced strength parameters, somewhat overestimates the load ratio compared with a non-associative model with full soil strength parameters. The discrepancy between the two models increases with the increase in the depth of the trapdoor and can be as much as 21%.

Acknowledgements

References

[1] Engesser, Fr. (1882). Ueber den Erdduck gegen innere Stützwande (Tunnelwande)." Deutsche Bauzeitung 1882; (16): 91–93 (in German).

[2] Terzaghi K. Stress distribution in dry and in saturated sand above a yielding trap-door. Proc., 1st Int. Conf. Soil Mech. Found. Eng. 1936; Vol. 1, Graduate School of Engineering,Harvard Univ., Cambridge,MA, 307–311.

[3] Ladanyi, B., Hoyaux, B. A study of the trap-door problem in a granular mass. Can. Geotech. J. 1969; 6(1): 1–15.

[4] Evans, C. H. An examination of arching in granular soils. S.M. thesis, Dept. of Civil Engineering, MIT, Cambridge, MA. 1983.

[5] Tanaka, T. and Sakai, T. Progressive failure and scale effect of trap-door problems with granular materials. Soils Found. 1993; 33(1):11-29.

[6] McNulty, J. W. An experimental study of arching in sand. Ph.D. thesis, Dept. of Civil Engineering, Univ. of Illinois, Urbana, IL. 1965.

[7] Abdulla, W. A., Goodings, D. J. Study of sinkholes on weakly cemented sand, Centrifuge 94, Balkema, Rotterdam 1994; 797-802.

[8] Stone, J.K. , Muir Wood, D. Effects of dilatancy and particle size observed in model tests on sand. Soils Found. 1992; 32(4): 43-57.

[9] Costa, Y. D., Zornberg, J. G., Bueno, B. S., Costa, C. L. Failure mechanisms in sand over a deep active trapdoor. ASCE J. Geotech. Geoenviron. Eng. 2009; 10.1061/ (ASCE) GT.1943-5606.0000134, 1741–1753.

[10]   Iglesia, G. R. Trapdoor experiments on the centrifuge: A study of arching in geomaterials and similitude in geotechnical models." Ph.D. thesis, Dept. of Civil Engineering, MIT, Cambridge, MA. 1991.

[11]   Iglesia, G.R., Einstein, H.H., Whitman, R.V. Investigation of soil arching with centrifuge tests. ASCE J Geotech Geoenviron Eng 2014; 140(2): 04013005.

[12]   Dewoolkar, M. M., Santichaianant, K., Ko, H.-Y. Centrifuge modeling of granular soil response over active circular trapdoors. Soils Found. 2007; 47(5): 931– 945.

[13]   Rui, R., van Tol, A. F., Xia, Y.-y., van Eekelen, S. J. M., Hu, G. Investigation of soil-arching development in dense sand by 2D model tests. Geotech. Test. J. 2016; 39(3): 415–430.

[14]   Jacobsz, S. W. Trapdoor experiments studying cavity propagation. Proceedings of the First Southern African Geotechnical Conference 2016; pp.159-165. DOI: 10.1201/b21335-30.

[15]   Iglesia, G.R., Einstein, H.H., Validation of centrifuge model scaling for soil systems via trapdoor tests. ASCE J Geotech Geoenviron Eng 2011; 137(11): 1075-1089.

[16]   Terzaghi K. Theoretical soil mechanics. John Wiley and Sons Inc; 1943.

[17]   Bierbaumer, A. Die dimensionerung des tunnelmauerwerks, Engelmann, Leipzig, Germany; 2013.

[18]   Krynine D P. Discussion of 'Stability and stiffness of cellular cofferdams', by Karl Terzaghi. Trans. Am. Soc. Civ. Eng. 1945; 110: 1175–1178.

[19]   Rui, R., van Tol, A. F., Xia, Y.-y., van Eekelen, S. J. M., Hu, G. Evolution of Soil Arching: 2D Analytical Models. Int. J. Geomech. 2018; 18(6): 04018056.

[20]   Davis, E. H. Theories of plasticity and the failure of soil masses. In Soil mechanics: selected topics (ed. I. K. Lee) 1968; pp. 341-380. London: Butterworths.

[21]   Gunn, M. J. Limit analysis of undrained stability problems using a very small computer. Proceedings of the symposium on computer applications in geotechnical problems in highway engineering, Cambridge 1980; pp. 5-28.

[22]   Martin CM. Undrained collapse of a shallow plane-strain trapdoor. Géotechnique 2009; 59(10):855–63.

[23]   Smith, CC. Limit loads for an anchor/trapdoor embedded in an associative Coulomb soil. Int. J. Numer. Anal. Meth. Geomech. 1998; 22(11): 855–865.

[24]   Smith, CC. Limit loads for a shallow anchor/trapdoor embedded in a non-associative Coulomb soil. Géotechnique 2012; 62(7): 563–571.

[25]   Sloan SW, Assadi A, Purushothaman N. Undrained stability of a trapdoor. Géotechnique 1990; 40 (1):45–62.

[26]   Wang L, Leshchinsky B, Evans TM, Xie Y. Active and passive arching stresses in c'-ϕ' soils: A sensitivity study using computational limit analysis. Comput Geotech 2017; 84: 47–57.

[27]   Smith C, Gilbert M. Application of discontinuity layout optimization to plane plasticity problems. In: Proceedings of the royal society of London a: mathematical, physical and engineering sciences, vol. 463(2086). The Royal Society; 2007. p. 2461–84.

[28]   Koutsabeloulis, N. C., and Griffiths, D. V. Numerical modelling of the trapdoor problem. Geotechnique1989; 39(1): 77–89.

[29]   Nakai T, Wood DM, Stone KJL. Numerical calculations of soil response over a displacing basement. Soils Found 1995; 35(2): 25-35.

[30]   Dassault Systèmes. ABAQUS analysis user's manual. Simulia Corp., Providence, R.I. 2017.

[31]   Belytschko T, Liu W K, Moran B. Nonlinear Finite Elements for Continua and Structures, Wiley-Blackwell. 2000.

[32]   Sloan, S. W. Lower bound limit analysis using finite elements and linear programming. Int. J. Numer. Analyt. Methods Geomech. 1988 ; 12(1): 61–67.

[33]   Bolton, M.D. The strength and dilatancy of sands. Géotechnique 1986; 36(1): 65-78.

[34]   Drescher A, Detournay E. Limit load in translational mechanisms for associative and nonassociative materials. Géotechnique 1993; 43(3): 443–456, http://dx.doi.org/10.1680/.